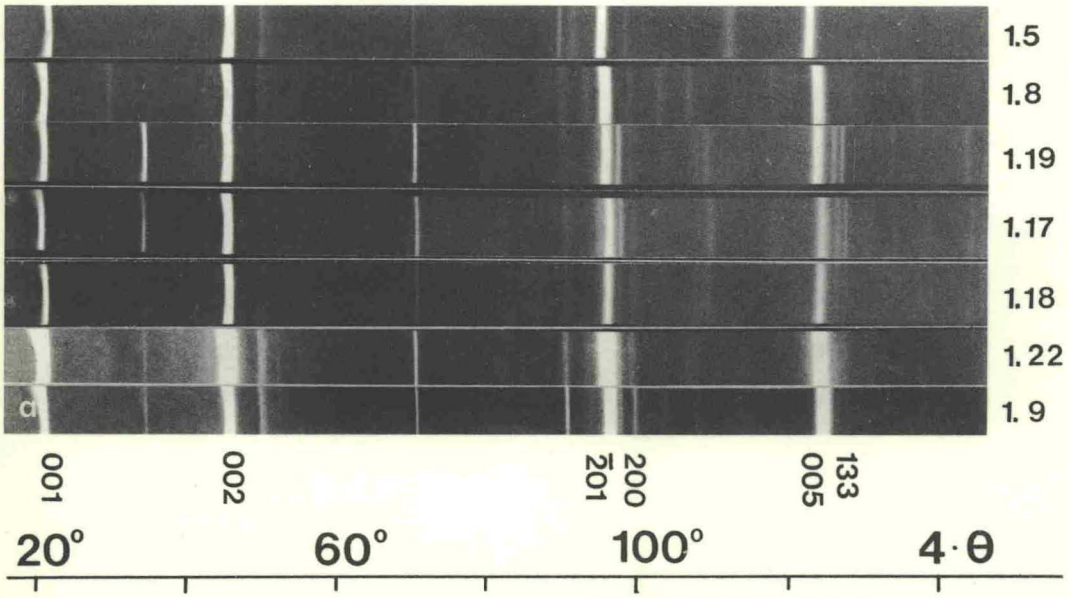
1.5
1.8
1.19
1.17
1.18
1.22
1.9
a
001
002
201
200
005
133
20°
60°
100°
4·θ

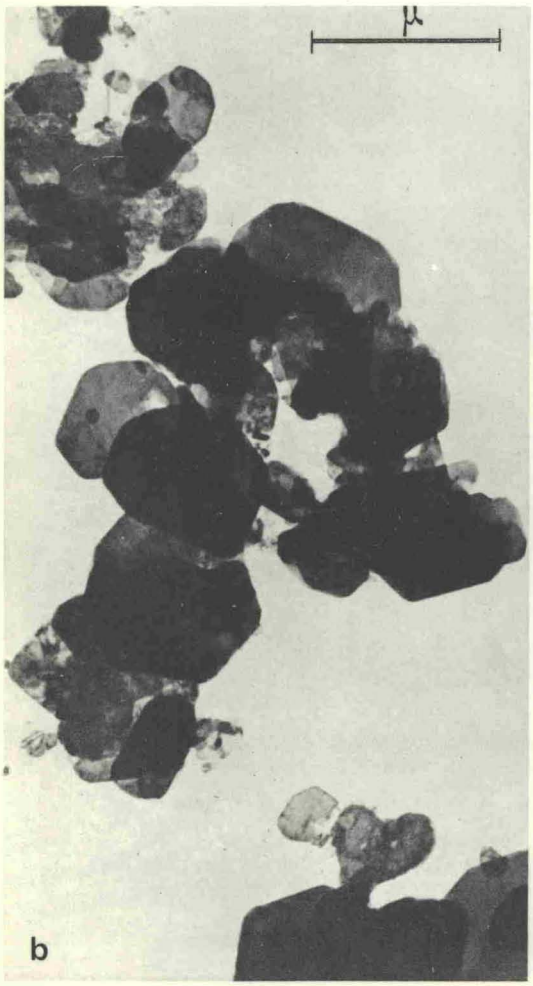
b


c

Plate II

Fig. a. — Selected area electron diffraction of synthetic lithiophorite single crystal. An idealized drawn pattern is shown in Figure 1 in the text.

Fig. b. — Typical product of series 2 (No. 2.9). Carbon replica, Cr shadowed; ×15,000.

Fig. c. — Needle shaped by-product in sample No. 2.8. Direct preparation; ×15,000.

Fig. d. — Same, but carbon replica, Cr shadowed; ×25,000.

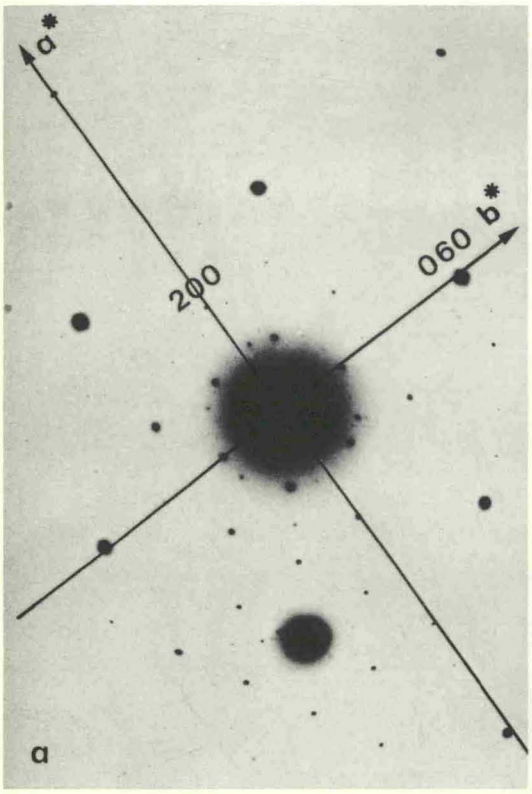
a*
200
060 b*
a

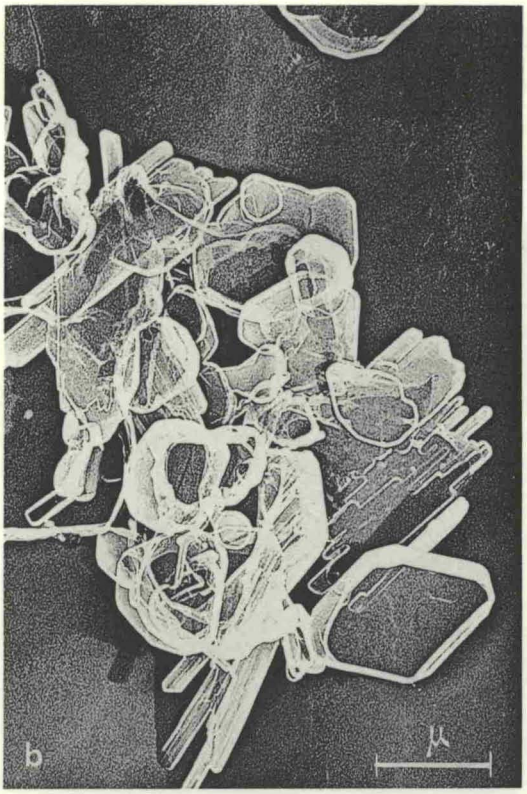
b
μ

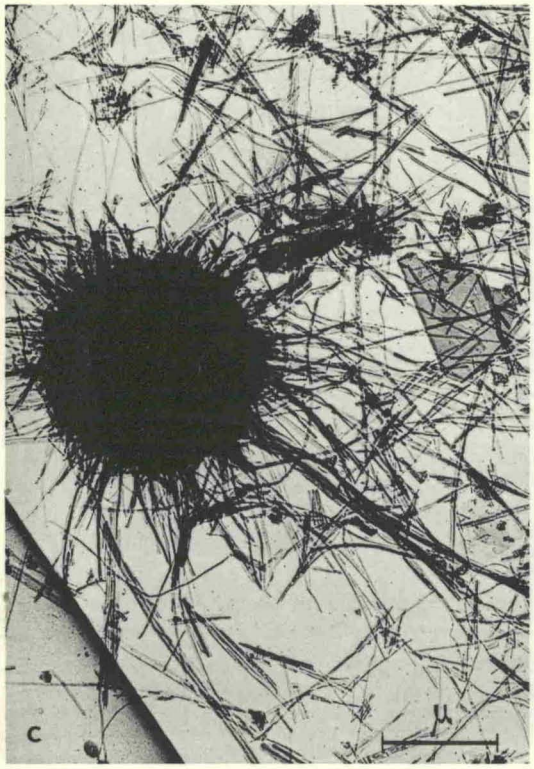
c
μ


d

Plate III

Fig. a. — X-ray pattern of isolated by-product in sample 2.5, and schematic representation of literature reference pattern of γ-AlOOH.

Fig. b. — Na^+ substituted preparation typical for series 2 as fig. *b* on Plate II, but direct preparation. Sample 2.5. ×12,000. $LiAl_2Mn_3O_9 \cdot 3\,H_2O$ can not be distinguished from γ-AlOOH.

Fig. c. — Selected area electron diffraction of γ-AlOOH single crystal isolated from sample No. 2.5 (fig. *b*).

Fig. d. — Selected area electron diffraction of by-product in series 2, forming rafts of needles (fig. *e*).

Fig. e. — By-product typical for Na^+ containing preparations (series 2). Electron diffraction with streaks perpendicular to direction of needles is shown in fig. *d*; ×15,000.

Fig. f. — Same, but carbon replica, Cr shadowed; ×15,000.

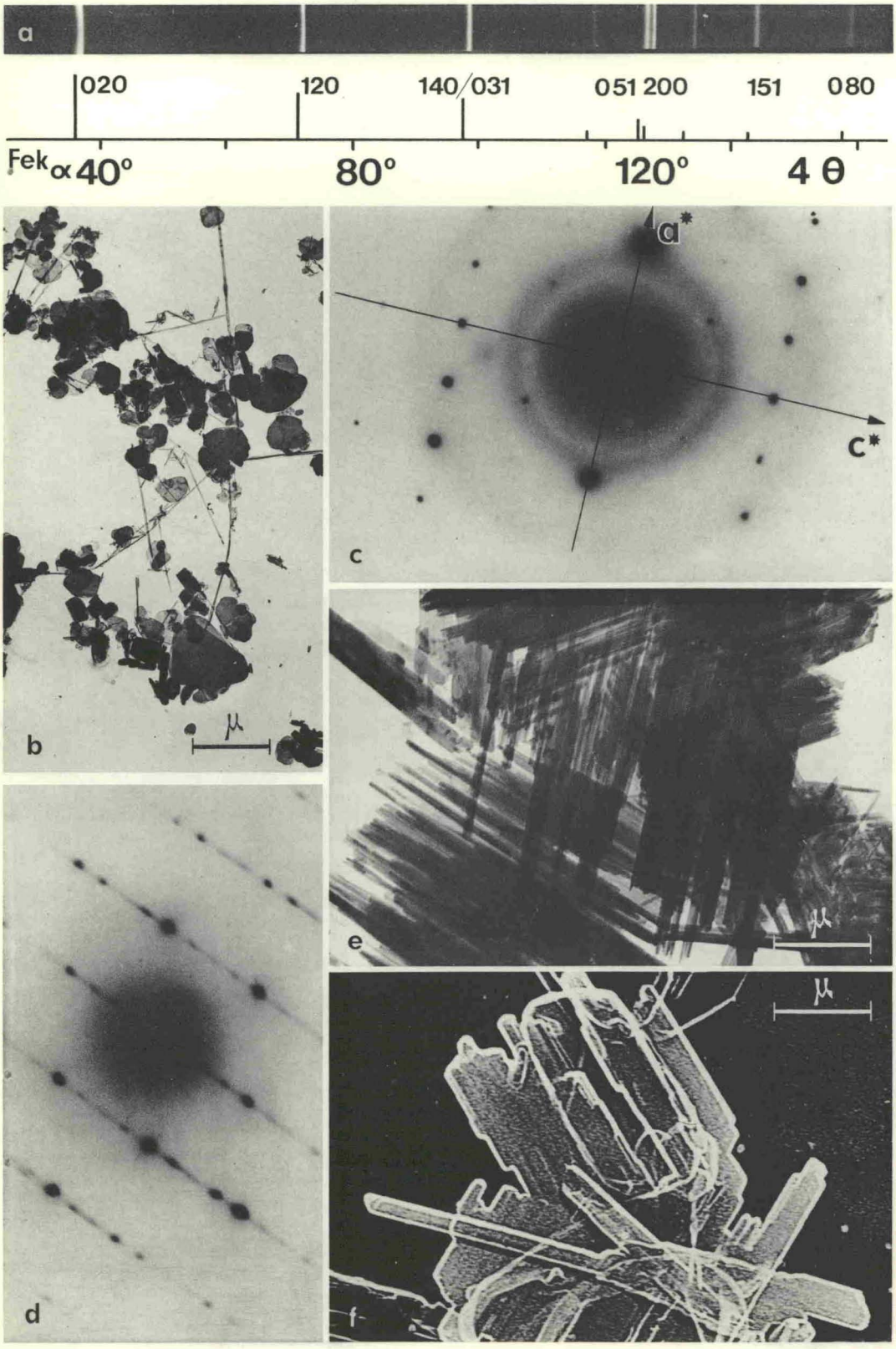
a
020
120
140/031
051 200
151
080
Fek α 40°
80°
120°
4 θ
b
μ
a*
c*
c
e
μ
μ
f
d

Plate IV

Fig. a. — X-ray patterns of series 2, containing Na^+. Samples with γ-MnO_2 as starting material. Top: Pure $LiAl_2Mn_3O_9.3H_2O$ (No. 1.5) for comparison. Samples numbered according to Table 2. Na^+ and Li^+ contents in atom-%, from top:

0 % Na	10 % Li
2	8
5	5
8	2
9,6	0,4

Fig. b. — X-ray patterns of series 2, samples with $Mn_7O_{13}.5H_2O$ as starting material. Top: Pure $LiAl_2Mn_3O_9.3H_2O$ (No. 1.5) for comparison. Samples numbered according to Table 2. Na^+ and Li^+ contents in atom-%, from top :

0 % Na	10 % Li
2	8
3	7
5	5
7	3
9	1
10	0

Fig. c. — X-ray patterns of series 3. Top: Pure $LiAl_2Mn_3O_9.3H_2O$ (No. 1.5) for comparison. Samples numbered according to Table 3. Zn^{2+} and Al^{3+} contents in atom-%, from top:

0 % Zn	20 % Al
3	17
7	13
9	11
10	10
12	8
14	6
20	0

Fig. d. — Evaluation of sample No. 3.17 (0 % Al): X-ray patterns of No. 3.17, $K_{2-x}Mn_8O_{16}$ (above), $ZnMn_2O_4$ and ZnO (below).

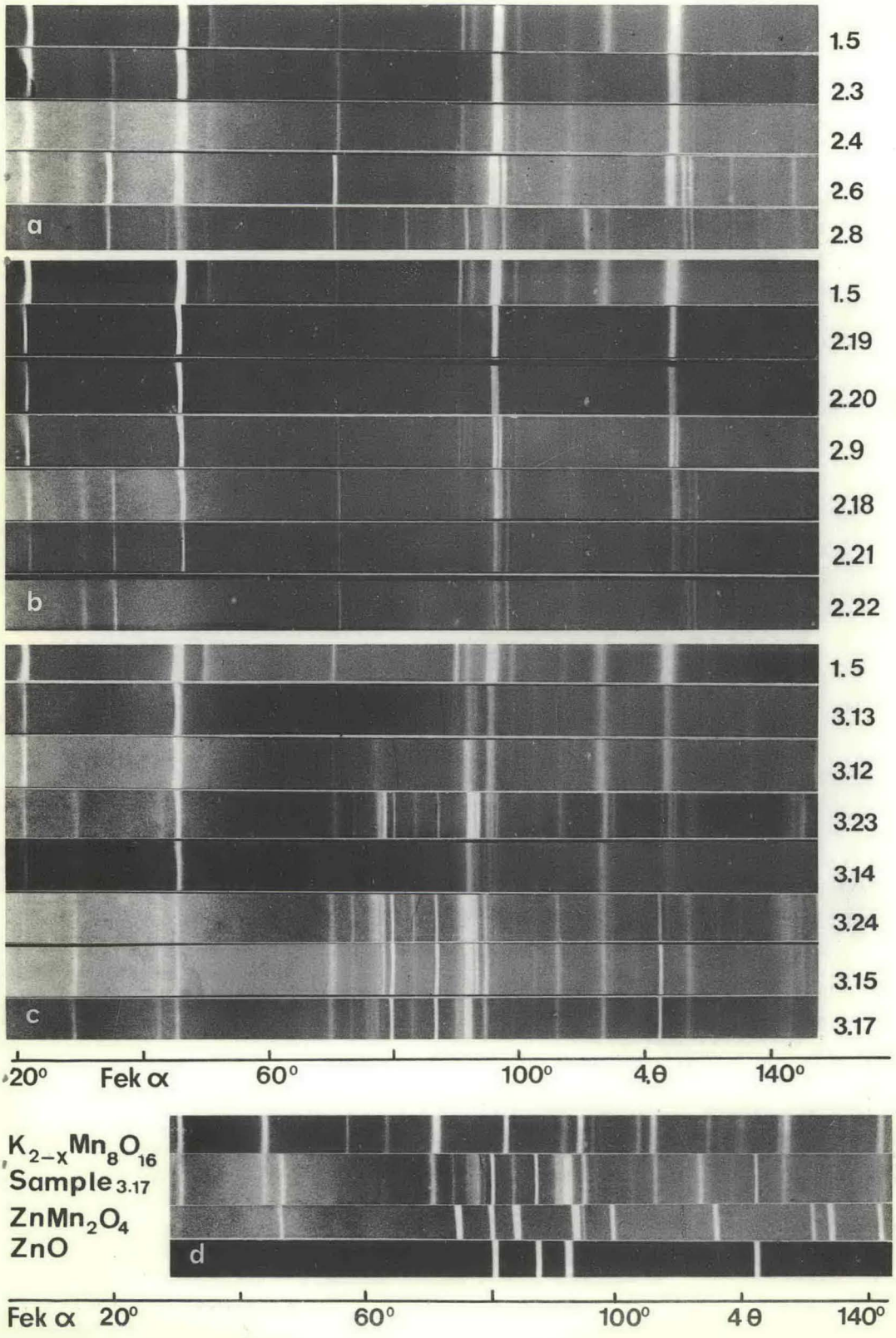

JOURNAL DE MICROSCOPIE

R. Giovanoli and coll.

Plate IV

Separatum of *Chimia* 28 (1974) fasc. 4
Monatsschrift des Schweizerischen Chemiker-Verbandes
Sauerländer AG, CH-5001 Aarau (Schweiz)

43

Dehydration of γ-FeOOH: Direct Observation of the Mechanism *

Summary

The dehydration of γ-FeOOH to γ-Fe_2O_3 has been investigated by thermoanalytical, electron microscopic and X-ray diffraction methods, using single crystals of suitably small size as a starting material, in order to maintain short diffusion paths. While kinetical data alone are not conclusive, the electron micrographs show unambiguously how the reaction proceeds in the crystals: Strings of perfectly oriented γ-Fe_2O_3 crystallites of about 70 Å diameter and disordered lithium site vacancies extend into the undecomposed matrix crystal which can be distinguished from decomposed parts by direct imaging of the (120) lattice planes of 3 Å spacing. An atomistic interpretation of this result is given.

* Received March 13, 1974.

1 Introduction

A comprehensive study of reactions involving solids should, in our opinion, include formal kinetics as well as morphological, textural and structural investigations. In order to exclude the influence of the surface, there is a tendency to use fairly large crystals. Under such conditions, however, diffusion paths are too long and will *eo ipso* influence the reaction mechanism. Such kinetic data, however good, will thus be of little help to decide between several possible mechanisms. FEITKNECHT[1] has pointed out that *small* single crystals will be the most suitable substrate to investigate solid state reactions. Only one reaction, however, has been studied along these lines, namely the oxidation of Fe_3O_4 to γ-Fe_2O_3[2,3].

We have studied a basically different reaction, i.e. the thermal decomposition 2 γ-FeOOH→ γ-Fe_2O_3 + H_2O. The relations between the two lattices involved are well known[4,5]. More recently GALLAGHER[6] has concluded from spectroscopic investigations that the γ-FeOOH lattice contains a considerable percentage of molecular water due to the peculiar arrangement of the OH...O bonds which yields, through a temperature dependent equilibrium, water molecules already at room temperature.

2 Experimental

γ-FeOOH was prepared by adding 0,15 L $FeCl_2$ 0,2 M to 0,1 L H_2O and 0,1 L NH_3/NH_4Cl buffer (*p*H 7,5), and introducing air at a rate of 0,5 L/min at 50 C in a waterbath. To maintain *p*H 6, NH_3 0,1 M was added dropwise from a buret (about 0,66 L altogether) while the *p*H was observed continuously with a glass electrode. After about 2 h the suspension proved free of Fe^{2+} (*o*-phenthroline test), i.e. the reaction was completed. The yellow-brown precipitate was isolated in a centrifuge, washed, and dried at 60 C. Its BET surface was about 14 m^2/g.

For X-ray diffraction a de Wolff-Guinier camera and FeK_α radiation were used. Reflection profiles from a Philips-Norelco goniometer served to calculate crystallite size and lattice disorder. Direct observation of the crystals was undertaken using a Siemens Elmiskop I, a Hitachi HU-11 A, and a Hitachi HU-12 A electron microscope.

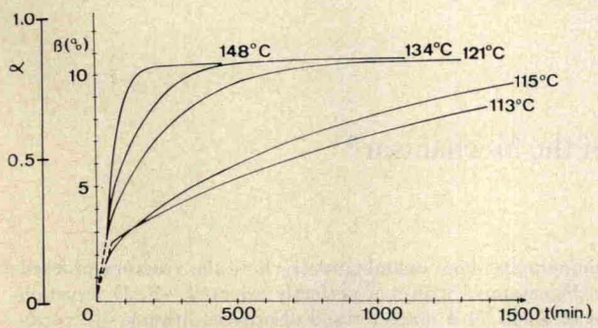

Fig. 1. Set of isothermal decomposition runs of γ-FeOOH. Abscissa: Time as measured, in minutes. Ordinates: β = weight loss in percent, before correction for adsorbed water. α = Reaction rate going from 0 to 1 (or 0 to 100%) without corrections

Unisothermal and isothermal decomposition was produced on a Mettler Thermoanalyzer TA 1 *in vacuo* (about 10^{-5} torr). Pt–Rh (10%) crucibles of 3, 12 and 16 mm diameter were used, with sample thickness not exceeding a few tenths of a mm. Evacuation and, under unisothermal conditions, heating rates, were as small as possible.

3 Results

Fig. 1 represents a typical set of decomposition curves under isothermal conditions. The reaction always ended sluggishly, and some residual water cannot be removed at all unless α-Fe_2O_3 nucleates.

When such results are plotted in a coordinate system with reduced time scale ($t/t_{½}$) on the abscissa and reaction rate 0 to 1 on the ordinate, fig. 2 results.

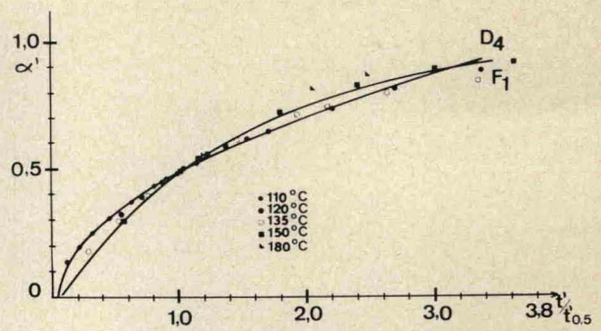

Fig. 2. Reduced time representation, after correction for adsorbed water, for isothermal decomposition of γ-FeOOH. The data used are a set different form that in fig. 1. Two calculated curves for different mechanism models from fig. 7 are also shown. α' = corrected reaction rate from 0 to 1 (or 0 to 100%)

The X-ray powder patterns of the samples undergoing decomposition (not shown here) are superpositions of the initial γ-FeOOH, with sharp reflections vanishing towards the end of the reaction, and of the γ-Fe_2O_3 pattern with extremely broad reflections. The profile analysis yields a crystallite size of the order of 70 Å and strong evidence for disorder, most probably in the vacant Lithium sites. It thus seems obvious that the tetragonal superlattice reflections of γ-Fe_2O_3 do not appear.

Electron micrographs of partly decomposed crystals show peculiar contrast phenomena which might be explained by strings of pores. As the crystals produce perfectly oriented electron diffraction textures (not shown here), these strings must be crystallites of γ-Fe_2O_3. Undecomposed crystals and, in partly decompo-

[1] W. FEITKNECHT, *Pure Appl. Chem. 9* (1964) 423.
[2] W. FEITKNECHT and U. MANNWEILER, *Helv. Chim. Acta 50* (1967) 570.
[3] K. J. GALLAGHER, W. FEITKNECHT and U. MANNWEILER, *Nature 217* (1968) 1118.
[4] J. D. BERNAL, D. R. DASGUPTA and A. L. MACKAY, *Nature 180* (1957) 645.
[5] D. R. DASGUPTA, *Ind. J. Physics 35* (1961) 401, and: T. TAKADA, M. KIYAMA and S. SHIMIZU, *Bull. Inst. Chem. Res. Kyoto Univ. 42* (1964) 505.
[6] K. J. GALLAGHER and D. N. PHILLIPS, unpublished.

Fig. 3. Electron micrograph of undecomposed γ-FeOOH showing (120) lattice planes of spacing 3,3 Å. Hitachi HU-12A. Magnification 5000000

sed platelets, the undecomposed regions, exhibit the usual extinction contours (Bragg fringes) which show that this part of the lattice is scattering coherently*. In a few cases it was possible to make directly visible the (120) lattice planes of γ-FeOOH in undecomposed crystals (fig. 3).

4 Discussion and conclusions

The kinetical data (fig. 2) fit equally well into quite different functions as shown in the representation of SHARP *et al.*[8] (Fig. 5). An unambiguous answer from these results alone, hence, is impossible.

The additional evidence from electron micrographs, X-ray diffraction, electron diffraction and BET surface measurements, however, suggests the following mechanism.

In order to form the γ-Fe_2O_3 lattice, the corrugated layers of edge and corner sharing (FeO_6) octahedra of γ-FeOOH must collapse in the manner shown schematically in fig. 6. By the introduction of more edge and corner sharing, O^{2-} ions in the form of water are set free. The considerable lattice strain visualized in fig. 6 accompanied by additional shear in the two other directions of the lattice leads to the total disruption of the dehydrated region of γ-FeOOH. The front of such a region being under strain is a suitable nucleus for further reaction; the process thus continues along the needle axis *c*, starting usually from cracks or other defects at the edge of the crystal. The strings of 70 Å large γ-Fe_2O_3 crystallites produce the mentioned contrast phenomenon since their neighbourhood has to support

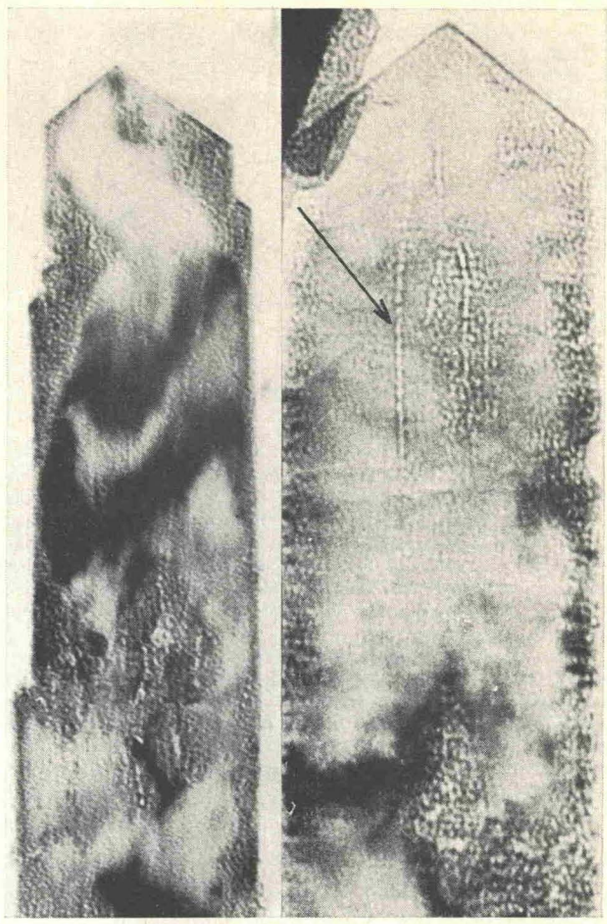

Fig. 4 Electron micrographs of partly decomposed γ-FeOOH crystals. Uniform grey regions with black extinction contours (Bragg fringes) are unaltered; the granular structure of other regions indicates complete dehydration. Instead of a sharp phase boundary, pearl-like strings intrude from decomposed regions into regions of unaltered γ-FeOOH. The visible crystallite size is consistent with 70 Å found from X-ray reflection profiles. BET measurements of the specific surface show that these features are not pores; hence they are crystallites of γ-Fe_2O_3 producing a considerable strain on the surrounding matrix, thus giving the contrast phenomenon. Arrow indicates strings of γ-Fe_2O_3. Magnification 200000

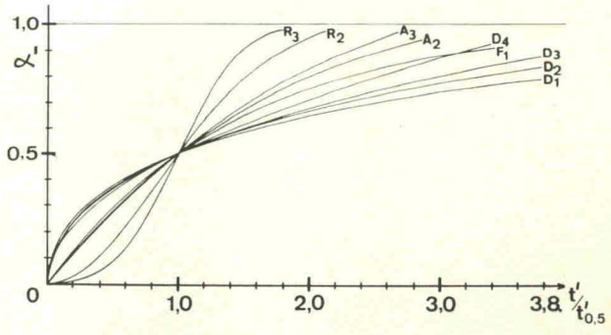

Fig. 5. Calculated rate curves representing various models of reaction mechanisms, after SHARP *et al.*[8] Reduced time scale and ordinate as fig. 2. *F* 1 = First order law (Random nucleation), *D* 1 to 4 = diffusion controlled mechanisms, *A* = Avrami equations, *R* = boundary controlled mechanism. For full explanation see reference [8]

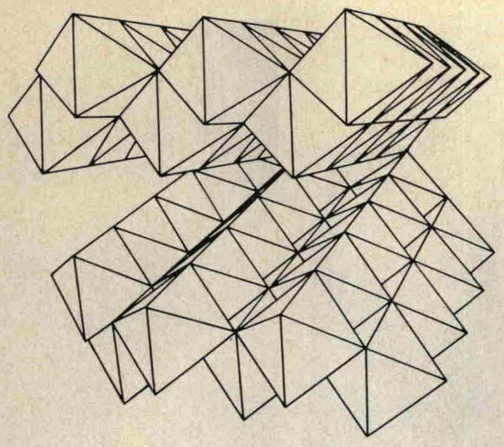

Fig. 6. Schematic three-dimensional representation of interface between undecomposed γ-FeOOH and final γ-Fe_2O_3, producing the considerable strain in the γ-FeOOH crystal and the contrast effect in the electron micrograph. The front of the picture represents the boehmite type lattice of γ-FeOOH (hydrogen bonds holding together the corrugated layers are omitted). Towards the background these layers approach each other until they collapse (in the back end of the figure).

From there the octahedra would extend further backwards forming essentially a cubic dense packing, i. e. the γ-Fe_2O_3 lattice. This representation showing the transition between the two lattices makes evident the total disruption of the initial crystal into numberless microcrystallites consisting of only about 5 to 10 unit cells. It also makes evident that in these microcrystals ordering to the perfect γ-Fe_2O_3 structure is not possible.

considerable shear and other strain. The contrast is best visible in the early stage of the dehydration, when it shows particularly well against the Bragg fringes uf the surrounding undecomposed matrix.

The final product has still a crystallite size of 70 Å. The residual water is therefore chemisorbed and cannot take off even *in vacuo*, hence the sluggish end part of the reaction. This might lead to the erroneous conclusion that γ-Fe_2O_3 is stable only in the presence of protons. FEITKNECHT[1, 2] and GALLAGHER[3] have, however, shown that this view is incorrect.

The small crystallite size and the low temperature seem to suppress the rearrangement of the lattice disorder, as opposed to the ordering observed in γ-Fe_2O_3 cubes of about 30 times larger size in O_2 atmosphere.

A full account on this subject will be submitted to *Thermochimica Acta*.

We thank Professor W. FEITKNECHT and Dr. K. J. GALLAGHER for helpful discussions, Dr. H.-G. WIEDEMANN (Mettler Ltd). for permission to use apparatus and for other support, Mr. T. KAMINO for help to obtain lattice resolution, Miss ETTINGER for photographic work, and the Swiss National Fund for financial support.

RUDOLF GIOVANOLI und RUDOLF BRÜTSCH

Laboratory of Electron Microscopy
Institute of Inorganic Chemistry
University of Berne
Freiestrasse 3
P.O.B. 140, CH-3000 Berne 9 (Switzerland)

* Bragg fringes are bands in which the Bragg condition for diffraction is fulfilled and where coherently scattered parts of the electron beam are caught at the contrast aperture. Such "extinction contours" are therefore dark[7].

[7] L. REIMER, *Elektronenmikroskopische Untersuchungs- und Präparationsmethoden*, 2nd Edition, Springer, Berlin 1967, p. 191 ff.

[8] J. H. SHARP, G. W. BRINDLEY and B. N. NARAHARI ACHAR, *J. Amer. Ceram. Soc. 49* (1966) 379.

Separatum of *Chimia* 27 (1973) fasc. 3
Monatsschrift des Schweizerischen Chemiker-Verbandes
Printed in Switzerland
Sauerländer AG, CH-5001 Aarau

37

Chromium(III)hydroxide hydrate—a new hydroxide structure type with cross-linked hydrogen bonding*

Summary

Precipitation of hexaquo chromium(III) solutions with OH^- ions yields a hydroxide with analytical composition $Cr(OH)_3 \cdot 3H_2O$ of the anti-bayerite type. The lattice constants of the pseudo-hexagonal unit cell are $a_0 = 5{,}047$ and $c_0 = 4{,}73$ Å. This lattice has vacancies where bayerite would have occupied octahedral sites, and *vice versa*, in a hexagonal closest arrangement of OH^- and H_2O. It consists of layers of isolated $[Cr(OH_2)_3(OH)_3]$ units. These are held together by a network of two kinds of hydrogen bonds. IR evidence gives O . . . HO distances of 2,7 and 2,9 Å, respectively. Precipitation experiments with $H_2{}^{18}O$ enriched solvent could be explained by a simple and fast deprotonation mechanism where the inner coordination sphere of the hexaquo chromium (III) ion remains unaltered. Upon ageing an amorphous phase of undefined composition is formed, where corner and/or edge sharing of hexaquo chromium (III) octahedra occurs. The solubility rate of this aged product in acids is distinctly lower, as the inner coordination sphere of the Cr^{3+} has to be attacked.

1. Introduction

As known since the investigations of FRICKE[1] and HANTZSCH and TORKE[2] the precipitation of hexaquo chromium (III) solutions with hydroxide ions yields a phase of analytical composition $Cr(OH)_3 \cdot 3H_2O$. BACCAREDDA and BEATI[3] found that diffraction data point to a bayerite type lattice, an opinion maintained up to now[4]. This lattice, however, cannot accommodate the three hydrate waters. We have reproduced the early experiments and try in this present investigation to interpret analytical, X-ray, and IR data and to put forward a mechanism for the formation of this new lattice.

2. Experimental

A freshly prepared 0,1 N $Cr(NO_3)_3 \cdot 9H_2O$ solution was precipitated with a stoichiometric amount of 0,1 N ammonia at room temperature. The product was isolated by centrifuging, washed five times with water and dried in air. By a similar procedure a small portion of $Cr(OH)_3 \cdot 3H_2O$ was prepared using ^{18}O enriched water, $H_2{}^*O$, as a solvent. Care was taken that only a negligible amount of $H_2{}^*O$ entered the inner coordination sphere of the hexaquo chromium (III) ion prior to the precipitation of $Cr(OH)_3 \cdot 3H_2O$[5]. The X-ray powder pattern of this hydroxide was identical with that of the normal $Cr(OH)_3 \cdot 3H_2O$. The ^{18}O abundances in the reactant solutions of chromium (III) nitrate and ammonia and in the washing water were determined by mass spectrometry using the CO_2 exchange technique[6]. Similarly, the hydroxide was exchanged with CO_2 in sealed quartz tubes by heating for 20 hours at 350 °C. A cycloidal mass spectrometer CEC 21-620 A, kindly provided by the Federal Institute of Reactor Research (Würenlingen), was used for the isotope analysis. X-ray powder patterns were taken on a Guinier-de Wolff camera using copper radiation. An aluminium foil 0,08 mm thick directly in front of the film absorbed the fluorescence radiation of Cr. Infrared spectra were recorded on a Beckman IR-9 spectrometer in KBr pellets, Nujol mull, and Fluorolube mull.

* Received February 14, 1973.

3. Results

The following ^{18}O abundances were found (atom %):

Mother liquid after precipitation	2,85
0,1 N $Cr(NO_3)_3$ solution before precipitation	2,85
0,1 N ammonia before precipitation	2,84
$Cr(OH)_3 \cdot 3H_2O$	0,519
Last (fifth) portion of washing water	0,250

The IR spectra showed two distinct OH stretching frequencies (fig. 1), a narrow one at about 3500 cm^{-1} and a fairly broad one at about 3000 cm^{-1}. The first can be attributed to a rather long OH ... O bond, of the order of about 2,9 Å while the second points to a distinctly shorter hydrogen bond of the order 2,7 Å. For comparison we refer to NAKAMOTO *et al.*[7]. The shape of the second mentioned stretching frequency happens to be quite similar to that of diaspor α-AlOOH[7].

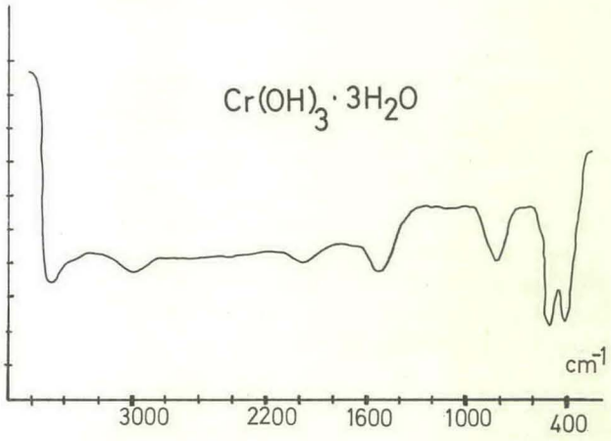

Figure 1. IR spectrum of chromium (III) hydroxide hydrate. Fluorolube mull technique

The X-ray powder pattern could be indexed with a pseudo-hexagonal unit cell using $a_0 = 5{,}047$ and $c_0 = 4{,}73$ Å as lattice constants. Four lines remained unexplained and suggest a super-cell. The appearance of the powder pattern is that of the bayerite type.

4. Discussion

The isotope analysis of the mother liquid and the solid hydroxide shows that $H_2{}^*O$ essentially remains in the aqueous phase. The small enrichment left in the hydroxide can be explained by uncomplete removal of mother liquid from the finely divided solid. In such cases the washing process tends to be tedious ; thus, after the fifth washing a slightly higher abundance of $H_2{}^*O$ in the water was still detectable (0,250 instead of 0,197 atom ‰).

It can be assumed that the inner coordination sphere of Cr^{3+} remains unaltered during the crystallisation process of the hydroxide. This fact and the stoichiometry of the precipitate suggest strongly that the following deprotonation takes place:

$$[Cr(OH_2)_6]^{3+}_{aq} \rightarrow [Cr(OH_2)_3(OH)_3]_s + 3\,H^+_{aq}$$

The $[Cr(OH_2)_3(OH)_3]$ units crystallise to a close packed arrangement as drawn out schematically in fig. 2 *.

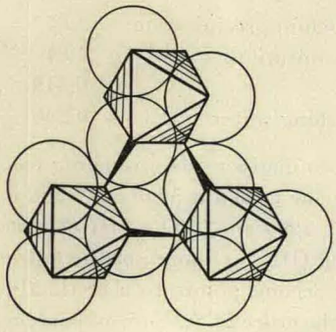

Figure 2. Part of a layer of the proposed anti-bayerite lattice for chromium (III) hydroxide hydrate. Circles represent oxygen ions. Protons and the next oxygen layer are omitted. Octahedra represent Cr^{3+} positions slightly above the plane of the drawing. Three black spikes indicate hydrogen bonds of the first of the two different sets

Fig. 2 shows part of a layer of close packed OH^- ions and water molecules. Octahedral sites occupied by Cr^{3+} ions are symbolised by octahedra. Some hydrogen bonds of one of the two sets mentioned are drawn. If this picture is carried on, an arrangement similar, but inverse, to the bayerite type lattice appears: sites occupied in this type are vacant in chromium (III) hydroxide hydrate, and *vice versa*. We propose to call this arrangement "anti-bayerite type".

* We wish to point out that we are indebted to Professor G. Schwarzenbach, Zurich, for having given us the crucial idea to this interpretation.

Since the mentioned units are essentially isolated in this arrangement (as opposed to bayerite where edge, corner and face sharing OH^- octahedra hold the lattice together), it seems obvious to take the IR evidence into consideration and to assume a cross-linked hydrogen bond network. One OH ... O bridge is shown in fig. 2, but another kind must also exist as per Cr^{3+} unit six more protons are available for bonding.

On ageing or by heating (even under water), chromium (III) hydroxide hydrate turns into a totally amorphous phase of undefined composition, and of distinctly deeper green colour. This is probably due to condensation of the isolated octahedral units to corner or edge sharing dimers or higher polynuclears. Under these circumstances no lattice order whatsoever beyond the first neighbour is detectable.

If polynuclears have had time to form in the Cr^{3+} solution, the simple deprotonation mechanism does not lead to the crystalline hydroxide. The latter dissolves readily in acids as opposed to the amorphous product where the inner coordination sphere of the Cr^{3+} ion must be attacked. This is further support to the anti-bayerite type described above.

A full account on this new hydroxide structure will be published elsewhere.

Acknowledgments. Authors are grateful to Professor W. Feitknecht for the suggestion to investigate this hydroxide, to Professor G. Schwarzenbach for valuable discussions, to Mr. P. Bürki for preparative work, to Mr. O. Antonsen (Federal Institute of Reactor Research, Würenlingen) for mass spectrometric measurements, and to the Swiss National Foundation for financial support.

Rudolf Giovanoli, Willy Stadelmann and Heinz Gamsjäger

Institute of Inorganic Chemistry of the University of Berne, Freiestrasse 3, P.O.B. 140, CH-3000 Berne 9 (Switzerland)

1 R. Fricke, *Z. anorg. allg. Chem. 132* (1924) 273.
2 A. Hantzsch und E. Torke, *Z. anorg. allg. Chem. 209* (1932) 60.
3 M. Baccaredda and E. Beati, *Atti del X° Congresso Internazionale di Chimica, Roma 1938*, vol. 2, p. 99.
4 ASTM card No. 16-817 (new name: JCPDS, or Joint Committee for Powder Diffraction Standards).
5 J. P. Hunt and H. Taube, *J. Chem. Physics 19* (1951) 602; R. A. Plane and H. Taube, *J. Physic. Chem. 56* (1952) 33; J. P. Hunt and R. A. Plane, *J. Amer. Chem. Soc. 76* (1954) 5960.
6 P. Baertschi, *Helv. Chim. Acta 36* (1953) 1352.
7 K. Nakamoto, M. Margoshes and R. E. Rundle, *J. Amer. Chem. Soc. 77* (1955) 6480.